2001

Mixing in Curved Pipes

Marco Latini
Harvey Mudd College

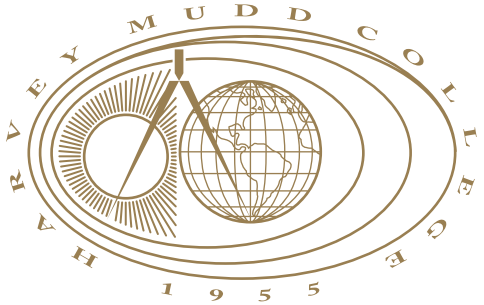

Mixing in Curved Pipes

by
Marco Latini
Andrew J. Bernoff, Advisor

Advisor: _____

Second Reader: _____

(Mario Martelli)

May 2001

Department of Mathematics

HARVEY MUDD
COLLEGE

Abstract

Mixing in Curved Pipes

by Marco Latini

May 2001

In this thesis we consider the problem of tracer dispersion in a toroidal pipe. It is known since the work by Dean in 1928 that flows in curved pipes present more challenges than flows in straight pipes. In fact the curvature induces a transverse recirculation in the form of outward spinning vortices. In this thesis we examine mixing associated with a point discharge release of tracer at the center of the spinning vortices. Plotting the longitudinal growth rate of the cloud of tracer, as measured by the standard deviation σ, as a function of time we were able to determine four regimes in the mixing process. For very small times we observed a growth rate consistent with diffusion where $\sigma \sim \sqrt{Dt}$. This is followed by a regime where $\sigma \sim D^{1/2}t^{3/2}$, consistent with an off-center release for a straight pipe. Then we observed a regime where $\sigma \sim Dt^2$, consistent with a centerline release for a straight pipe. This is due to the averaging effect of the longitudinal velocity by the recirculation that generates an effective parabolic velocity profile centered at the release point. Finally for large time we observe the Taylor regime with $\sigma \sim \sqrt{D_{eff}t}$. We also obtain the longitudinal profiles for the different regimes and find agreement with results for straight pipes.

Table of Contents

List of Figures

Acknowledgments

I would like to thank Prof. Andrew Bernoff for proposing this interesting problem and for mentoring me during this year. I also wish to thank Prof. Mario Martelli for helpful insights and suggestions on the problem. Finally a special thanks goes to Prof. Leslie Ward for her helpful suggestions on presentation skills. Finally I wish to thank the HMC mathematics department for its support.

Chapter 1

Introduction

In this thesis we characterize mixing in a toroidal pipe. The correspondent problem for straight pipes has received a lot of attention in the literature and its basic mechanisms are known since the revolutionary work by Taylor [14] in 1953 later extended by Aris [1] in 1956. Taylor and Aris were able to show that at large times, any initial configuration of tracer obeys a diffusion equation with a Gaussian distribution whose width grows diffusively. Recently Latini and Bernoff [9] examined the problem of a point discharge release of tracer at the center of the straight pipe. We were able to show that if we measure the longitudinal spread of the tracer, it is possible to observe a transient regime where this spread is growing faster than what expected by the action of diffusion alone. This non-diffusive growth is called anomalous diffusion. We were also able to characterize the longitudinal concentration profile in the anomalous regime by finding a new analytic self-similar solution.

In this thesis we extend these results to curved pipes. Flows in curved pipes present more challenges than flows in straight pipes since the curvature induces a transverse recirculation in the form of opposite outward spinning vortices. This transverse recirculation was first explained by Dean in 1928 [5]. The recirculation enhances mixing and explains why curved pipes are used in cooling systems and whenever heat exchanges become important.

Our analysis provides some insight into why the recirculation enhances mixing.

In fact if we release tracer at the center of the rotating lobes, the rotating lobes have the effect of averaging the longitudinal velocity along the streamlines and this creates an effective longitudinal parabolic profile. Thus release at the center of the rotating lobes becomes equivalent to release at the center of a straight pipe. This has the effect of a faster longitudinal spreading of the cloud of tracer as a result of the shear. We also investigate in this thesis the profiles associated with the regimes and we observe agreement with results for straight pipes.

1.1 Plan of the thesis

This section provides a guide to the chapters of this thesis. This first chapter is meant as a brief introduction to the problem. A more thorough introduction can be found in chapter two.

In the second chapter of this thesis we present the main results for mixing in straight pipes derived in our earlier work, see [9]. These results are significant because they enable us to understand our findings for curved pipes. The present work constitutes an important extension of Latini and Bernoff's previous results.

In the third chapter we introduce the physical model, a toroidal pipe, and the associated toroidal coordinate system. We then derive the governing equations for the flow and show how these equations model the transverse recirculation. We then study mixing in the cross-section by considering two different initial conditions. We model a release at the center of the pipe and then a release along the vertical line through one of the circular cross-sections. These runs provide insight into the importance of the transverse recirculation.

In the fourth chapter we discuss the numerical algorithm used to simulate mixing in curved pipes. The numerical scheme is a split step Monte-Carlo particle method first developed by Lingevitch and Bernoff in 1994 [11], and here adapted to simulate mixing in curved pipes.

In the fifth chapter we present the results for mixing in curved pipes with an initial release of tracer at the center of the two lobes. In the mixing process we can identify four different regimes each characterized by a different scaling law for the longitudinal growth rate σ of the cloud of tracer. We then show how these four regimes are consistent with our results for straight pipes and how the longitudinal profiles of the cloud of tracer are also consistent with findings for straight pipes.

Finally in the sixth chapter we briefly summarize the findings and we outline some future work on the problem.

Chapter 2

Mixing in straight pipes

Before we present our results for mixing in a toroidal pipe, we review fundamental results for mixing in straight pipes. These results are significant in this context because they provide a framework to understand the present work for curved pipes. Moreover, in later chapters we compare our findings for curved pipes to these results. The present work in many ways constitutes an extension of previous work on straight pipes and we refer the reader interested in the background of the current problem to [9].

In this chapter we show how for a point release in a straight pipe the mixing process can be divided into three distinctive regimes each characterized by an appropriate scaling law for the longitudinal growth-rate of the cloud of tracer measured by the standard deviation σ. We present both results for a release at the center of the pipe and for an off-center point release. In both cases we observe three regimes. However, the scaling laws for the intermediate regimes in the two runs are different as we go from $\sigma \sim t^2$ in the case of a center-line release to $\sigma \sim t^{3/2}$ for an off-center release. We also present an argument from [9] to explain this difference.

2.1 Straight pipes and Taylor dispersion

For mixing in straight pipes we consider as our physical model a cylindrical pipe with a circular cross-section of unit radius. The flow in a straight pipe for low Reynolds numbers is parabolic and is called *Poiseuille flow*. Figure 2.1 shows the

cylinder and the parabolic flow profile.

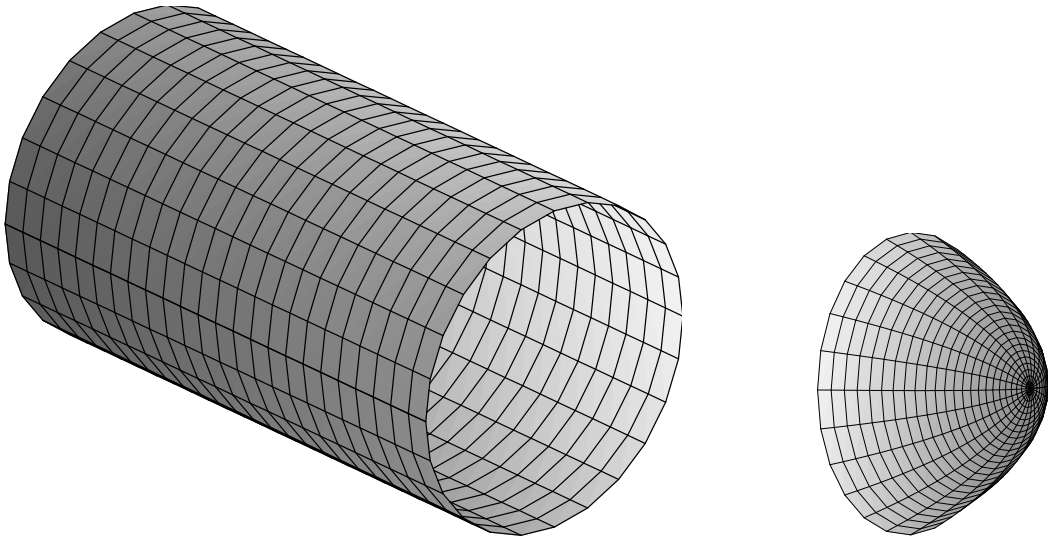

Figure 2.1: This figure represents the cylindrical pipe with the parabolic Poiseuille flow

The basic mechanisms of tracer dispersion in a straight pipe were first elucidated by the revolutionary work of Taylor in 1953 [14] and later extended by Aris in 1956 [1]. They concluded that any initial configuration of tracer will eventually assume a symmetric Gaussian distribution about a point moving with the mean velocity of the flow. Moreover, this symmetric distribution is spreading longitudinally according to a diffusion equation with an effective diffusivity constant $D_{eff} \propto 1/D$, where D is the diffusion coefficient and $D \ll 1$. This regime, which we call the *Taylor regime*, is achieved when all the tracer has become homogenized over the entire cross-section. If we consider the standard deviation σ as a measure of the longitudinal width of the cloud of tracer, Taylor observed that eventually the tracer is spreading longitudinally according to $\sigma \sim \sqrt{2D_{eff}t}$.

2.2 Anomalous diffusion and the anomalous regime

The problem of what happens before the Taylor regime was first addressed by Lighthill in 1966 [10]. Lighthill considered a uniform release of tracer in the cross-section of the pipe. He was able to characterize the shape of the longitudinal distribution of the tracer and was the first to observe that the tracer seemed to spread longitudinally according to $\sigma \sim t$. This would introduce a regime characterized by *anomalous diffusion* as the tracer is spreading faster than what expected by the action of diffusion alone.

Anomalous diffusion is observed in any phenomenon where the width of a distribution $\sigma(t)$ grows like t^γ with $\gamma \neq 1/2$. In particular if $\gamma > 1/2$, we have a super-diffusive process, otherwise if $\gamma < 1/2$ we have a sub-diffusive process. A super-diffusive process is an indication that the tracer is being spread faster than what expected by the action of diffusion alone. For more information on anomalous diffusion see the paper by Weeks et al [15].

2.3 The three regimes of shear dispersion

In our previous work on straight pipes [9], we considered a point discharge release of tracer and were able to identify three distinctive regimes for shear dispersion in laminar Poiseuille pipe flow. These three regimes are characterized by different scaling laws for the growth of the standard deviation $\sigma(t)$ of the tracer. We considered both a release at the center of the pipe and a release off-center. In both cases the mixing process is characterized by three regimes. We briefly present some physical arguments on the various regimes to motivate and explain our results. These results can also be derived analytically from the governing equations of the system. Again we refer the interested reader to our previous work.

Diffusive Regime. For small times after the release of the tracer, the longitudinal spreading caused by the action of diffusion is much larger than the effects of

the shear. This is due to the fact that the tracer is all concentrated at points moving with approximately the same velocity and thus any longitudinal spreading is mainly the result of diffusion. Thus for small times we would expect a diffusive regime since if we move into a reference frame together with the velocity at that point, the tracer obeys a diffusion equation and consequently spreads longitudinally according to $\sigma \sim \sqrt{2Dt}$.

Anomalous Regime. For intermediate times instead the longitudinal spread of the particles is mainly due to the effects of the shear. Particles are now located far apart along the cross-section and the separation caused by the difference in velocities is greater than the separation caused by the action of longitudinal diffusion. For this regime we find that the particles spread longitudinally according to $\sigma \sim t^{\gamma}$ with $\gamma > 1/2$. In particular for a point-discharge release of tracer at the center of the tube we have that $\sigma \sim \sqrt{8/3}\ Dt^2$ and for an off-center release we have $\sigma \sim \sqrt{8/3D}\ t^{3/2}$. Due to the non diffusive exponent this regime is called anomalous. We note that in this regime the particles have not interacted with the boundaries of the pipe.

Taylor Regime. At large times after the tracer has completely mixed over the entire cross-section of the pipe we achieve the Taylor regime. In the Taylor regime the different velocities of the particles over the cross-section are all averaged out to give a symmetric Gaussian configuration and if we move in a reference frame together with the average velocity, the tracer obeys a diffusion equation. Moreover, the tracer spreads longitudinally according to $\sigma \sim \sqrt{2D_{eff}t}$.

In our previous work we were able to characterize mixing in straight pipes according to these three different regimes.

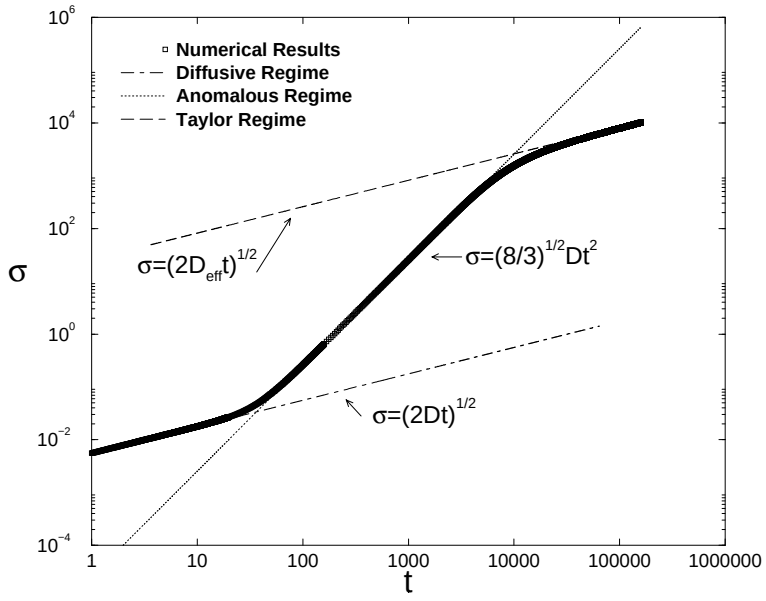

Figure 2.2: This figure illustrates the three stages of longitudinal dispersion observed for a center-line release of tracer in a straight pipe. The results are obtained for a value of $D = 1.625 \times 10^{-5}$.

2.4 Release at the center of the pipe

Figure 2.2 presents the three regimes observed for a point discharge release of tracer at the center of the pipe. The standard deviation σ is plotted as a function of time t in a log-log plot. A log-log plot is the most appropriate way to display the different regimes because different scaling laws correspond to straight lines with different slopes. Thus the three regimes are characterized by three straight lines with different slopes. Notice that the lines for the diffusive and anomalous regimes are parallel indicating that they have the same scaling law. Also notice the various time scales of the process. In particular notice that the transition between the diffusive and anomalous regime occurs at around time $D^{-1/3}$.

We can also plot the longitudinal profile of the tracer. For both the diffusive and Taylor regimes we observe a Gaussian distribution while for the anomalous regime

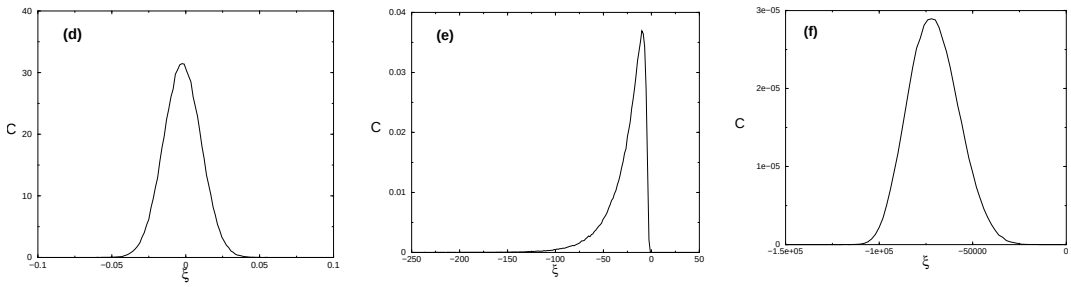

Figure 2.3: These figures show the longitudinal distribution for a point release at the center of a straight pipe in the three regimes. The figures are displayed in a reference frame moving with the centerline velocity $\xi = x - t$. Figure (d) and (f) show the Gaussian distribution corresponding to the diffusive and Taylor regimes. Figure (e) shows the asymmetric distribution corresponding to the anomalous regime.

we observe a peculiar asymmetric profile. This configuration is self-similar and in our previous work we found an analytical approximation to describe it, see [9]. Figure 2.3 presents the three longitudinal distributions observed from a reference frame moving together with the centerline velocity.

2.5 Off-center release

Figure 2.4 displays the three regimes for an off-center release at $r = 1/2$. Notice how we still have the three distinct regimes but this time the scaling law for the longitudinal width of the cloud of tracer in the anomalous regime is different. We went from a $\sigma \sim t^2$ to a $\sigma \sim t^{3/2}$.

We do not present the longitudinal distribution for this case because in all three regimes we observe a Gaussian distribution.

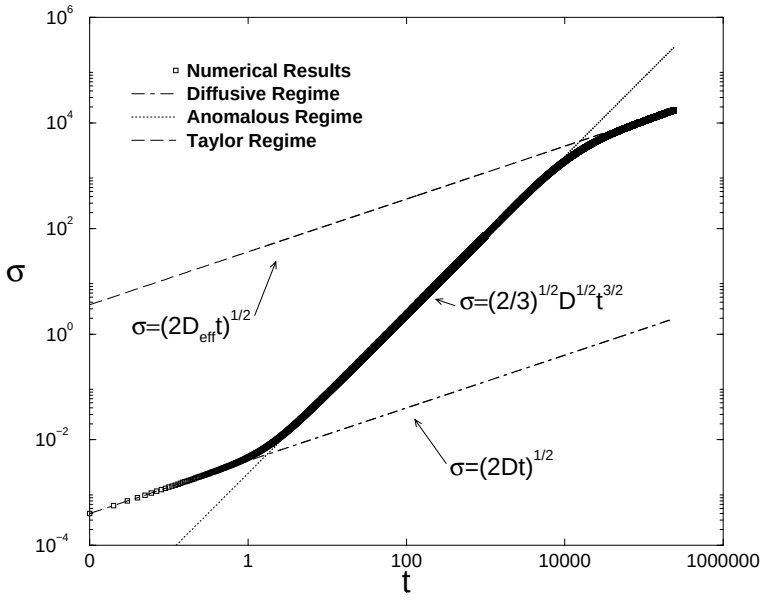

Figure 2.4: This figure illustrates the three stages of longitudinal dispersion observed for an off-center release of tracer in a straight pipe at $r = 1/2$. The results are obtained for a value of $D = 1.625 \times 10^{-5}$.

2.6 Computing the scaling laws and transition times

We now wish to investigate the scaling laws and the transition times between the various regimes observed.

To understand the scaling laws associated with the anomalous regime, we present an argument from [9]. "These results can be understood on dimensional grounds, following an argument given by [13]. Consider a point discharge in a Lagrangian frame moving with a parallel shear flow that scales locally as $(\Delta y)^n$ where Δy is the transverse displacement. After a time t, the tracer will have diffused transversely a distance proportional to $\sqrt{Dt}$. Consequently, the difference in velocity, Δv, between tracer in the center and the limb of the distribution will scale as $\Delta v \propto (Dt)^{n/2}$. Finally, the width of the distribution will scale as $\sigma \propto (\Delta v)t \propto D^{n/2}t^{n/2+1}$, in agreement with the Poiseuille flow results for release on the centerline ($n = 2$)

and away from the centerline ($n = 1$)".

The transition times between the diffusive regime and the anomalous can also be explained in a similar way. The transition between the two regimes occurs when the longitudinal displacement from diffusion, which we quantify as $\sqrt{Dt}$, is comparable to the displacement caused by the shear, which we quantify as $D^{n/2}t^{n/2+1}$. Thus this yelds $t \sim D^{(1-n)/(1+n)}$. For release on the centerline ($n = 2$) this yields a transition time $t \sim D^{-1/3}$. For release away from the centerline ($n = 1$), this yields $t \sim 1$.

Chapter 3

The toroidal pipe

Our study of mixing in curved pipe has concentrated mainly on the toroidal pipe because it is the simplest example of a curved pipe. This chapter introduces the coordinate system for a toroidal pipe and the governing equations for flows in toroidal pipes. These equations capture one of the most interesting physical effects observed in curved pipes, the transverse recirculation. The transverse recirculation is in the form of two outward spinning vortices. We also execute two test runs for a release at the center of the pipe and a uniform release along the y-axis. These two numerical runs serve to illustrate visually the process of mixing and show how the transverse recirculation affects mixing. In the next chapter we discuss the numerical code that was used to obtain these simulations.

3.1 The toroidal pipe and the toroidal coordinate system

Consider a curved pipe, as shown in figure 3.1 with a circular cross-section of unit radius. We introduce a toroidal coordinate system. So let R indicate the distance from the center of the torus to the center of the circular cross-section. We further introduce a polar coordinate system in (r, ϕ) to study the cross-section and we denote with θ the angular distance from the initial release in the curved pipe. Thus any particle inside the curved pipe will have coordinates (r, ϕ, s) where $s = R\theta$. Also note that we can easily express the position in terms of (x, y, s) where $x = r\cos\phi$ and $y = r\sin\phi$. Figure 3.2 illustrates the toroidal coordinate system used in this problem. In our model we wish to represent steady flow of water circulating in-

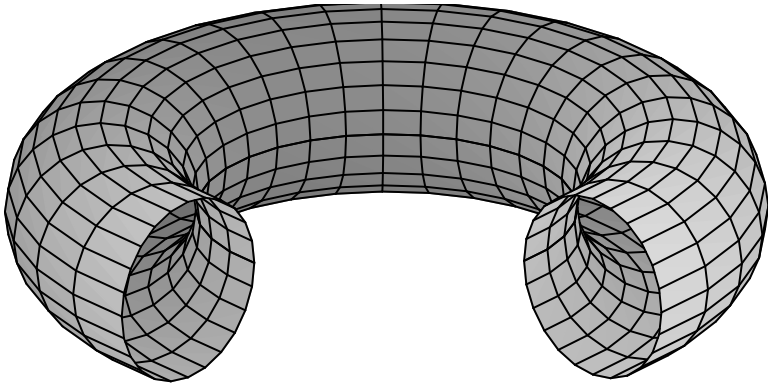

Figure 3.1: This figure illustrates a toroidal pipe

side this torus. At some specified time we release tracer according to some initial condition. Now it is a bit hard to imagine how one would get water flowing continuously inside a toroidal pipe but remember that our torus has small curvature (i.e. $R/a \gg 1$) thus we can imagine a torus with a very large R and we can apply a difference in pressure at the two ends to obtain our desired flow.

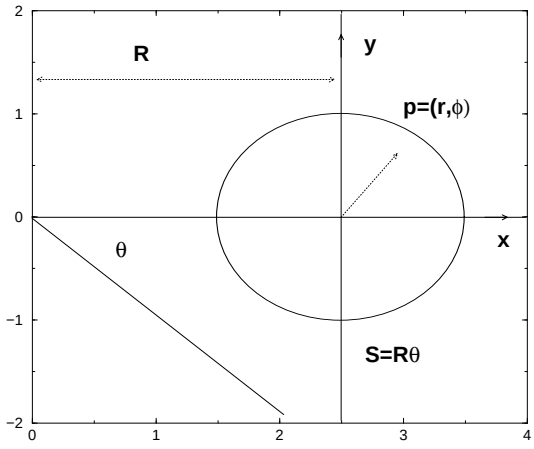

Figure 3.2: This figure represents the toroidal coordinate system used to study flows in curved pipes

3.2 Governing Equations

Consider a particle advected by the flow field, the three velocity components of the particle are (u, v, w), where u indicates the radial component, v the angular component and w the component in the s direction.

We can now write the full Navier-Stokes equations for flows in curved pipes. These equations describe how a particle moves in the pipe carried by the flow. Thus if we solved these equations for a specified initial position we could track the position and velocity of the particle as a function of time. Equations 3.1, 3.2, 3.3 and 3.4 represent the flow without imposing the condition that the flow be steady.

The Navier-Stokes equations for curved pipes are constituted by four equations. The first equation is called the continuity equation and represents an expression of the conservation of mass principle. The other three equation each express conservation of momentum for the u, the v and the w component. Conservation of momentum is another form of Newton's second law, and in this form it expresses the principle that a change in velocity must be caused by the action of some forces acting on the particle, such as a change in pressure or the action of surface tension.

The continuity equation can be written as:

$$\frac{\partial u}{\partial r} + \frac{u}{r}\frac{1 + 2\delta r\cos\phi}{1 + \delta r\cos\phi} + \frac{1}{r}\frac{\partial v}{\partial \phi} - \frac{\delta v \sin\phi}{1 + \delta r\cos\phi} + \frac{1}{1 + \delta r\cos\phi}\frac{\partial w}{\partial \phi} = 0. \tag{3.1}$$

The first conservation of momentum equation for the u direction can be written as:

$$\begin{aligned}\frac{\partial u}{\partial t} + u\frac{\partial u}{\partial r} + \frac{v}{r}\frac{\partial u}{\partial \phi} + \frac{w}{1 + \delta r\cos\phi}\frac{\partial u}{\partial s} - \frac{v^2}{r} - \frac{\delta w^2\cos\phi}{1 + \delta r\cos\phi} = \\ = \frac{\partial p}{\partial r} - \frac{1}{\mathrm{Re}}\left(\left(\frac{1}{r}\frac{\partial}{\partial \phi} - \frac{\delta\sin\phi}{1 + \delta r\cos\phi}\right)\left(\frac{\partial v}{\partial r} + \frac{v}{r} - \frac{1}{r}\frac{\partial u}{\partial \phi}\right) - \right. \\ \left. - \frac{1}{(1 + \delta r\cos\phi)^2}\frac{\partial^2 u}{\partial s^2} + \frac{1}{1 + \delta r\cos\phi}\left(\frac{\partial^2 w}{\partial r \partial s} + \frac{\delta\cos\phi}{1 + \delta r\cos\phi}\frac{\partial w}{\partial s}\right)\right).\end{aligned} \tag{3.2}$$

The second conservation of momentum equation for the v direction can be written

as:

$$\frac{\partial v}{\partial t}+u\frac{\partial v}{\partial r}+\frac{v}{r}\frac{\partial v}{\partial \phi}+\frac{w}{1+\delta r\cos\phi}\frac{\partial v}{\partial s}+\frac{uv}{r}+\frac{\delta w^2\sin\phi}{1+\delta r\cos\phi}= \\ =-\frac{1}{r}\frac{\partial p}{\partial \phi}+\frac{1}{\mathrm{Re}}\left(\frac{1}{(1+\delta r\cos\phi)^2}\frac{\partial^2 v}{\partial s^2}-\frac{1}{r(1+\delta r\cos\phi)}\frac{\partial^2 w}{\partial s\partial\phi}+\right. \\ \left.\frac{\delta\sin\phi}{(1+\delta r\cos\phi)^2}\frac{\partial w}{\partial s}+\left(\frac{\partial}{\partial r}+\frac{\delta\cos\phi}{1+\delta r\cos\phi}\right)\left(\frac{\partial v}{\partial r}+\frac{v}{r}-\frac{1}{r}\frac{\partial u}{\partial\phi}\right)\right). \quad (3.3)$$

The third Conservation of momentum equation for the w direction can be written as:

$$\frac{\partial w}{\partial t}+u\frac{\partial w}{\partial r}+\frac{v}{r}\frac{\partial w}{\partial \phi}+\frac{w}{1+\delta r\cos\phi}\frac{\partial w}{\partial s}+\frac{\delta uw\cos\phi}{1+\delta r\cos\phi}-\frac{\delta uw\sin\phi}{1+\delta r\cos\phi}= \\ =-\frac{1}{1+\delta r\cos\phi}\frac{\partial p}{\partial s}+\frac{1}{\mathrm{Re}}\left(\left(\frac{\partial}{\partial r}+\frac{1}{r}\right)\left(\frac{\partial w}{\partial r}+\frac{\delta w\cos\phi}{1+\delta r\cos\phi}\right)+\frac{1}{r^2}\frac{\partial^2 w}{\partial\phi^2}\right. \\ \left.-\frac{1}{r}\frac{\partial}{\partial\phi}\left(\frac{\delta w\sin\phi}{1+\delta r\cos\phi}\right)-\left(\frac{\partial}{\partial r}+\frac{1}{r}\right)\frac{1}{1+\delta r\cos\phi}\frac{\partial u}{\partial s}-\frac{1}{r}\frac{\partial}{\partial\phi}\left(\frac{1}{1+\delta r\cos\phi}\frac{\partial v}{\partial s}\right)\right) \quad (3.4)$$

We now impose the condition that the flow be steady, thus we eliminate the derivatives with respect to s except for the pressure components. Moreover, we assume that we are in a pipe with a slight curvature thus we have that $\delta = 1/R \ll 1$. This allows us to eliminate all the terms containing δ. For large curvatures the approximation is no longer valid and the equations of flow that we derive will accurately describe what is observed in a real pipe. After we apply this simplification, the continuity equation becomes:

$$\frac{\partial u}{\partial r}+\frac{u}{r}+\frac{1}{r}\frac{\partial v}{\partial\phi}=0, \quad (3.5)$$

the momentum equation in u becomes:

$$u\frac{\partial u}{\partial r}+\frac{v}{r}\frac{\partial u}{\partial\phi}-\frac{v^2}{r}-w^2\cos\phi=-\frac{\partial p}{\partial r}-\frac{2}{De\,r}\frac{\partial}{\partial\phi}\left(\frac{\partial v}{\partial r}+\frac{v}{r}-\frac{1}{r}\frac{\partial u}{\partial\phi}\right), \quad (3.6)$$

The momentum equation in v becomes:

$$u\frac{\partial v}{\partial r}+\frac{v}{r}\frac{\partial v}{\partial\phi}+\frac{uv}{r}+w^2\sin\phi=-\frac{1}{r}\frac{\partial p}{\partial\phi}+\frac{2}{De}\frac{\partial}{\partial r}\left(\frac{\partial v}{\partial r}+\frac{v}{r}-\frac{1}{r}\frac{\partial u}{\partial\phi}\right) \quad (3.7)$$

finally the momentum equation in w becomes:

$$u\frac{\partial w}{\partial r}+\frac{v}{r}\frac{\partial w}{\partial \phi}=-\frac{\partial p}{\partial s}+\frac{2}{De}\left(\left(\frac{\partial}{\partial r}+\frac{1}{r}\right)\frac{\partial w}{\partial r}+\frac{1}{r^2}\frac{\partial^2 w}{\partial \phi^2}\right) \tag{3.8}$$

Notice that the above equation can now be written as a function of only one parameter called the Dean number, defined as

$$De=\sqrt{\frac{a}{R}}\,\frac{2aW}{\nu}. \tag{3.9}$$

We can now find an analytical solution for this problem. For a more detailed derivation of eq. 3.10 see the papers by Berger et al [2] and Jones et al [8]. If we express the velocities (u,v,w) in terms of derivatives of the Cartesian coordinates $(\dot{x},\dot{y},\dot{s})$ then the solution to the Navier Stokes is given by:

$$\begin{aligned}\dot{x}&=\frac{\alpha}{1152}\left(h(r)+\frac{y^2}{r}\,\frac{\mathrm{d}h}{\mathrm{d}r}\right)\\ \dot{y}&=-\frac{\alpha}{1152}\,\frac{xy}{r}\,\frac{\mathrm{d}h}{\mathrm{d}r}\\ \dot{s}&=\frac{1}{4}\,\beta(1-r^2)\end{aligned} \tag{3.10}$$

where $h(r)=1/4\ (4-r^2)(1-r^2)^2$, $\alpha=DeC^2$ and $\beta=DeC/Re$, C is a constant representing the overall pressure and Re is the Reynolds number. Notice that we now have two parameters for the problem (α,β). Later for our numerical runs we introduce a third parameter D, the diffusivity constant.

These equations model a very important effect observed for flows in curved pipe, the transverse recirculation. The figure below shows a cross-section of the toroidal pipe and the transverse recirculation induced by the curvature.

We notice that the transverse recirculation is in the form of two outward spinning vortices. We also notice that the two vortices have a stagnation point located at approximately $y=\pm 0.4614$.

The recirculation greatly enhance mixing since the tracer will sample various velocities rapidly. This explains why curved pipes have many applications in cooling systems and other instances where heat exchanges are relevant. Moreover, one

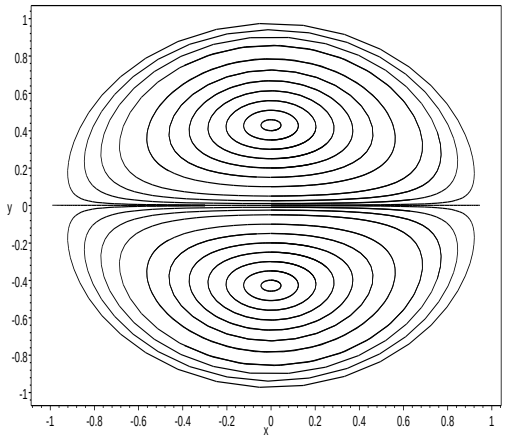

Figure 3.3: This figure illustrates the transverse recirculation observed in a cross-section of a toroidal pipe. Notice that the vortices are outward spinning.

could imagine the use of curved pipes in an industrial process to mix liquids. So instead of stopping the entire production process to put the liquids in a tank and mix them with a stirring device, one may just let the liquids flow in curved pipes.

3.3 Release at the origin

It is interesting to numerically simulate the transverse mixing of tracer released at the origin. This run physically corresponds to releasing a dot of dye at the center of the pipe. This run and the following run with a uniform release along the y-axis are motivated by the need for physical insight into the process of mixing in curved pipes. The simulation enables us to understand how strong and how effective the recirculation is and the time scales involved for a complete revolution around one of the close streamlines that make the recirculation.

Figures 3.4 and 3.5 follow in time the release of tracer at the origin as seen in the circular cross-section of the pipe. We obtain these figures by projecting all of the tracer onto a circular cross-section. Note however, that important physical

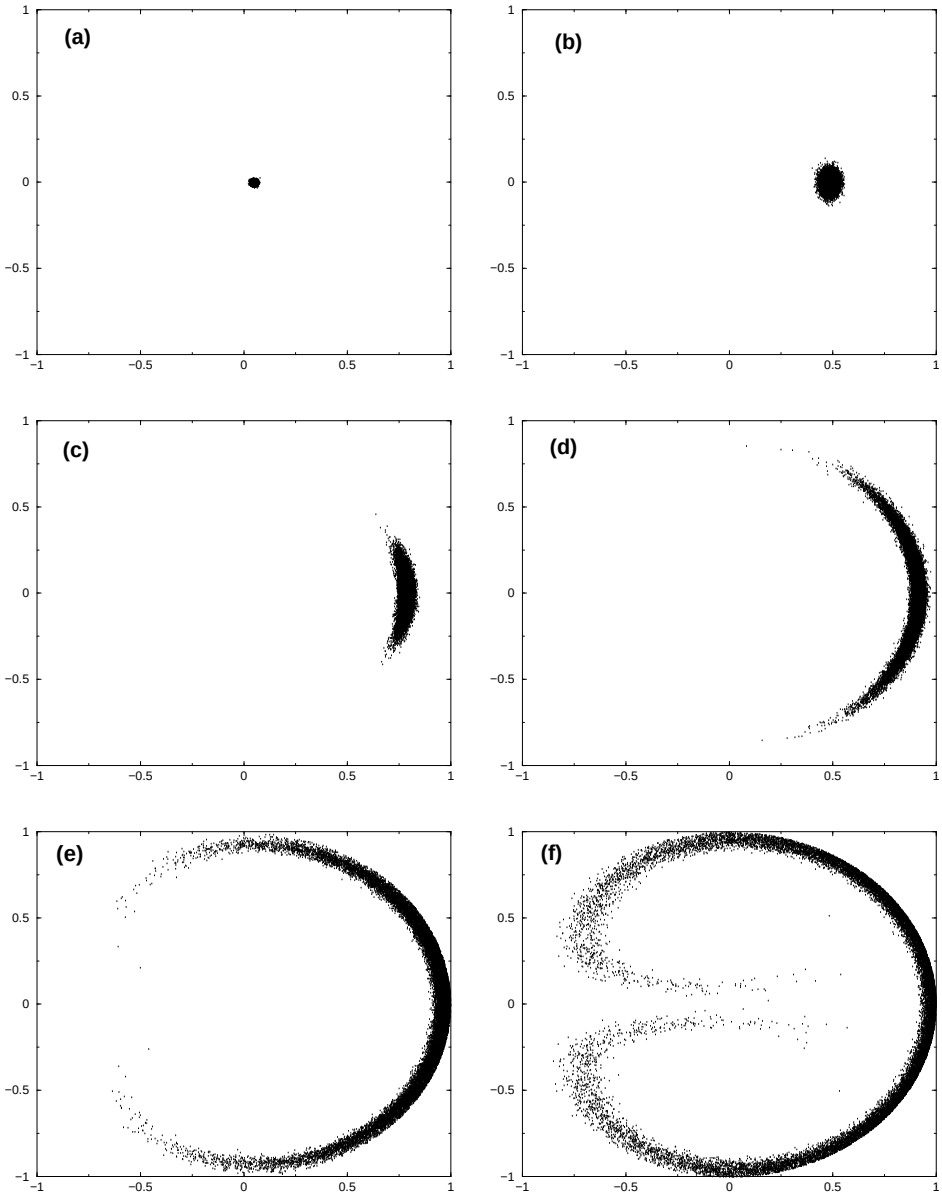

Figure 3.4: This figure illustrates transverse mixing in a toroidal pipe with a point release at the origin. The snapshots are taken at different times following the release. Figure (a) displays the tracer immediately after the release at $t = 0.1$, Figure (b) at $t = 1$, Figure (c) at $t = 2$, Figure (d) at $t = 3.5$, Figure (e) at $t = 6$, Figure (f) at $t = 9$. The numerical data is obtained for a diffusivity constant of $D = 0.0005$.

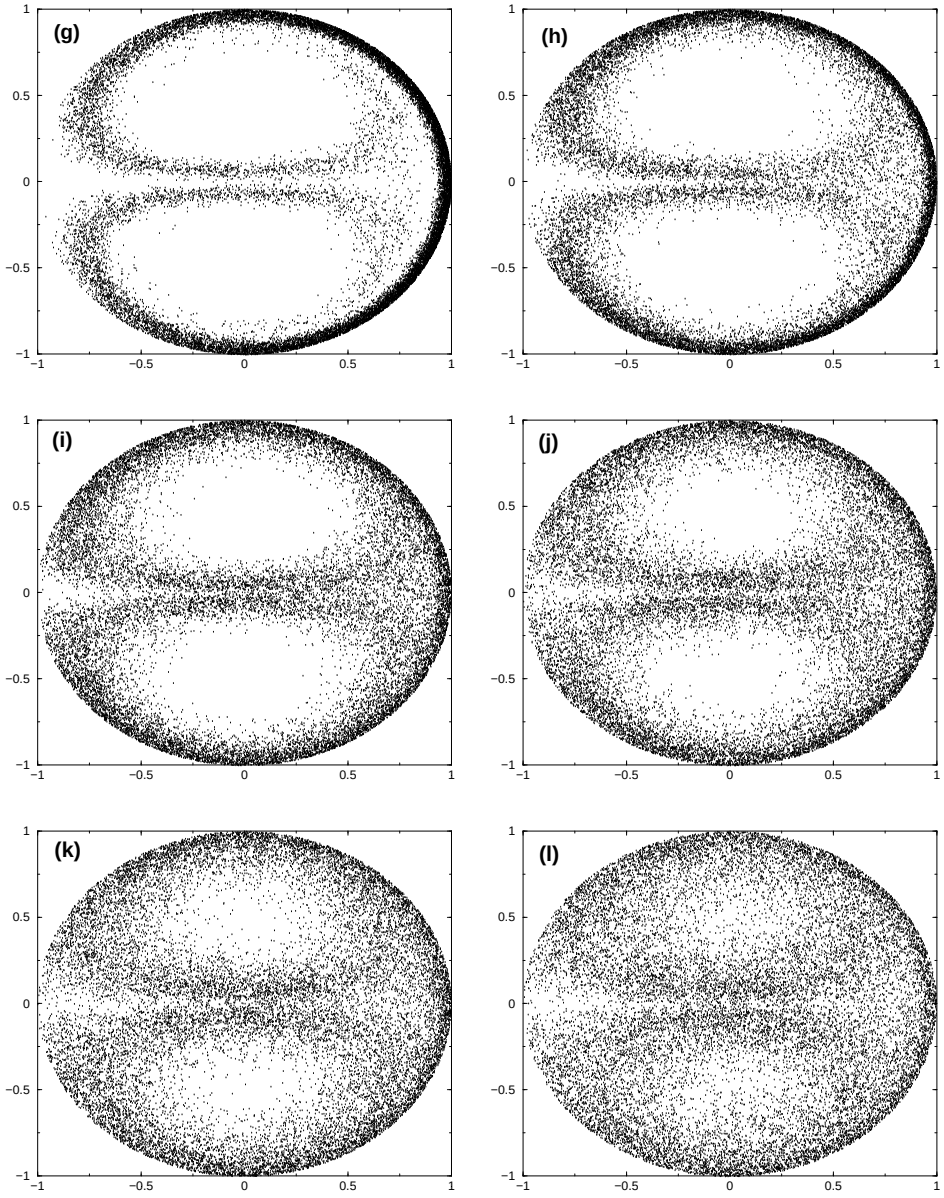

Figure 3.5: This figure illustrates transverse mixing in a toroidal pipe with a point release at the origin. The snapshots are taken at different times following the release. Figure (g) displays the tracer at $t = 13$, Figure (h) at $t = 18$, Figure (i) at $t = 25$, Figure (j) at $t = 40$, Figure (k) at $t = 60$, Figure (l) at $t = 100$. The numerical data is obtained for a diffusivity constant of $D = 0.0005$.

effects such as the longitudinal spreading and how rapidly the tracer is moving longitudinally are not visible through these runs. These quantities will be analyzed and their significance fully developed in the chapter where we consider mixing in a toroidal pipe.

As was predicted analytically (see figure 3.2 and equations 3.10) we observe transverse recirculation. These runs are obtained for a ratio of the outer radius of the torus R to the radius of the circular cross-section a equivalent to $R/a = 10$; note that the effects of the transverse recirculation are important even for a pipe where the ratio is very large, and thus for a torus with a small radius of curvature. Furthermore, we notice that, for the parameters relevant to this problem, namely the small diffusion limit, the cloud of particles hits the outer wall soon after the release of the tracer indicating that the circulation time for the particles is quite small. Notice also that the particles initially collect towards the outer wall of the pipe to form a thin layer over the entire outer wall. If we now think of the the tracer as being small particles carrying heat, this explains why curved pipes are relevant in heat exchanges problems. In fact as soon as the tracer hits the outer wall heat exchange can occur.

Another interesting result from this run is that particles are mixing from the outside to the inside of the two lobes towards the fixed points of the recirculating lobes. By time $t = 100$ the particles seem to have homogenized transversely thus we would expect the Taylor regime to be in place around this time for this initial condition.

3.4 Uniform release on a strip on the y-axis

We now consider a second simulation with a uniform release on the y-axis. This release is similar to releasing a thin strip of dye along the vertical axis of the curved pipe.

Figures 3.6 and 3.7 follow in time the evolution of the strip of dye on the cross-section. The strip is stretched by the recirculating flow in two opposite directions. The strip above the fixed point of the lobes is stretched toward the inside of the pipe, while the strip below the fixed point is stretched toward the outside of the pipe. This causes the "U" shape we observe for small times. Notice how the tracer pushed toward the outside of the pipe reaches the boundary soon after the release and also how a full circular spin around the lobes is obtained for a time t_r between three and four. In the chapter on mixing in curved pipes we fully develop and analyze the significance of t_r and the fact that t_r is quite small compared to the timescales of the various regimes observed in the mixing process.

From the figures we also see that, while the layer of tracer far away from the fixed points is stretched and becomes progressively thinner, the layer closer to the fixed points stays thicker. This is due to the fact that that with a uniform release, tracer closer to the center of the pipe has a greater distance to "circulate" than tracer closer to the fixed points.

Also notice how the full transverse mixing is achieved around time $t = 50$ and thus we would expect to observe the Taylor regime starting for this time scale.

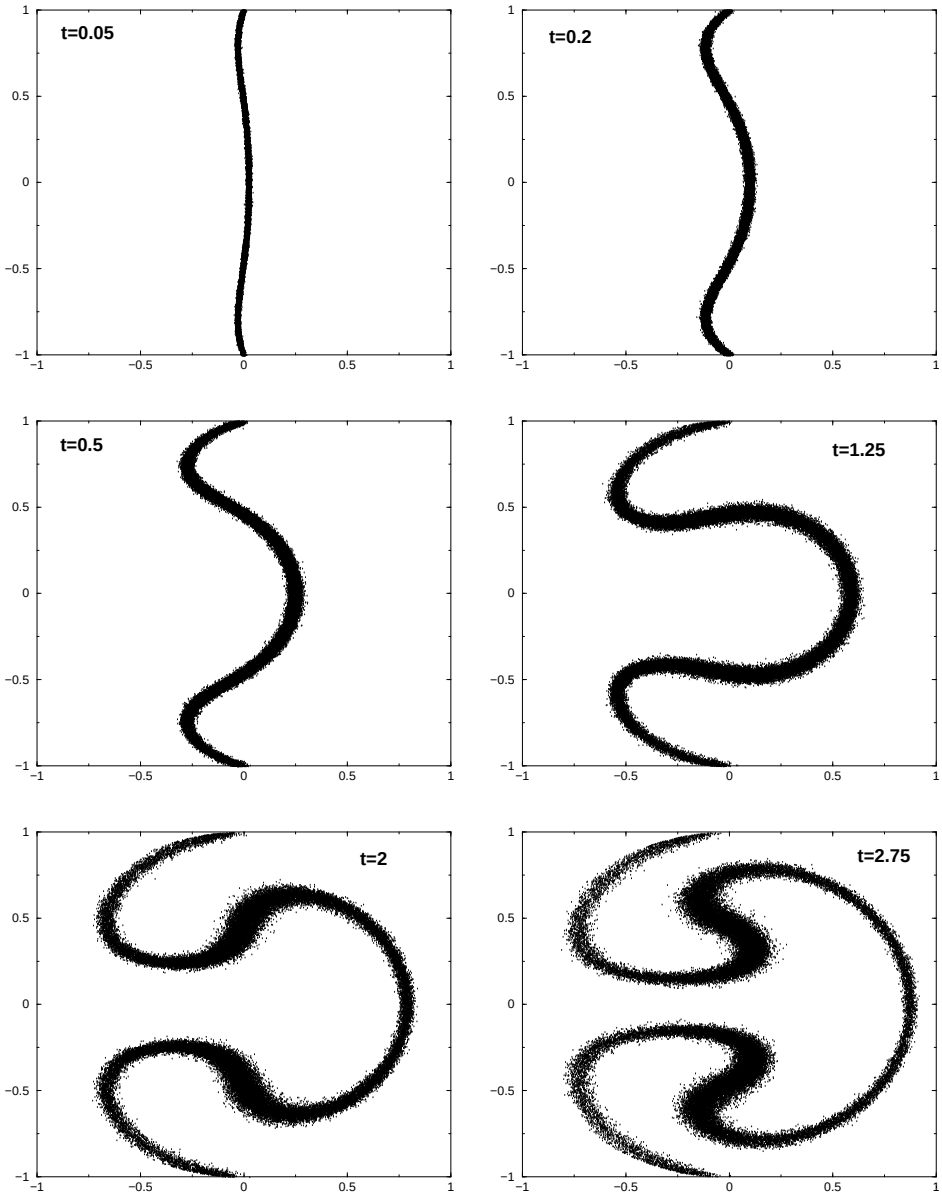

Figure 3.6: This figure illustrates transverse mixing in a toroidal pipe with a uniform release along the y-axis. The snapshots are taken at different times following the release.

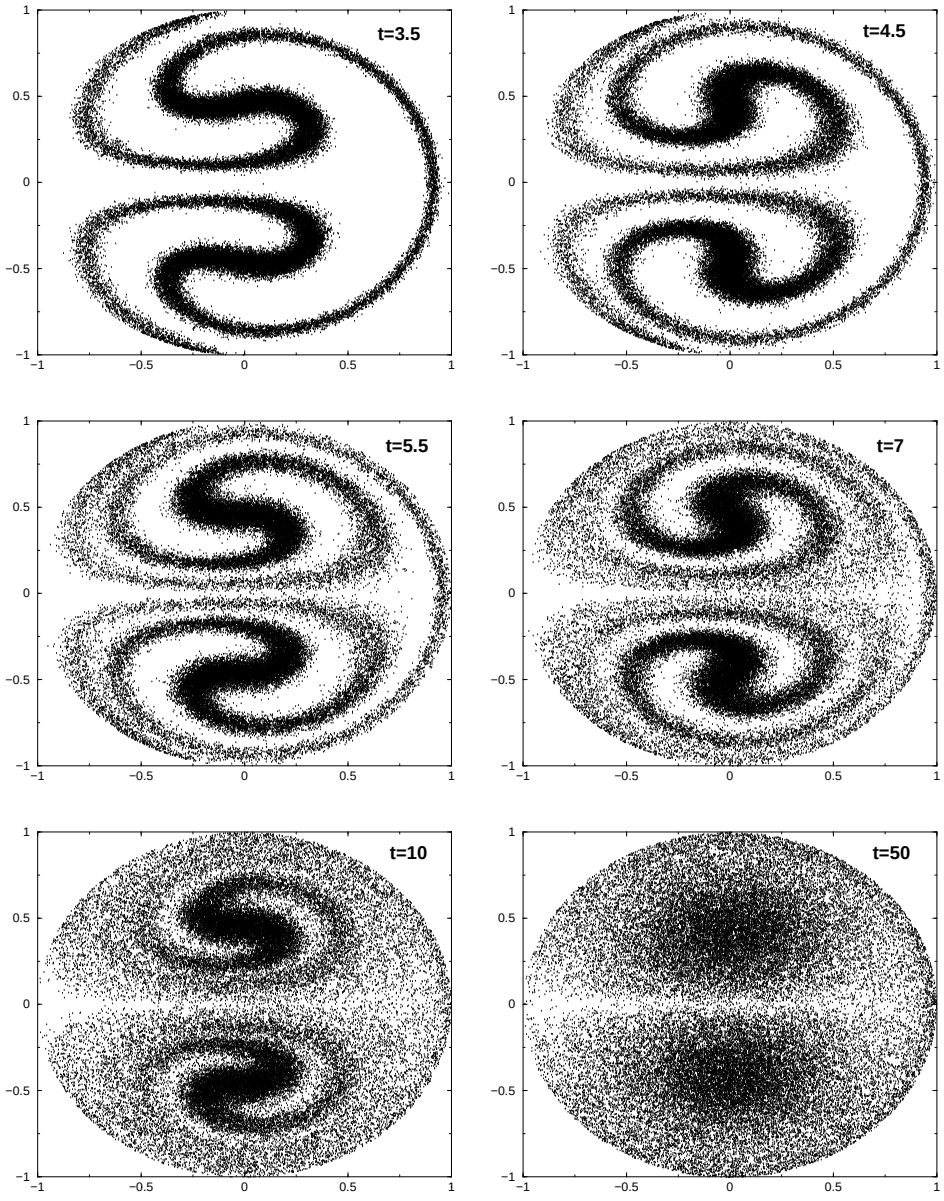

Figure 3.7: This figure illustrates transverse mixing in a toroidal pipe with a uniform release along the y-axis. The snapshots are taken at different times following the release.

Chapter 4

Numerics

The goal of this chapter is to provide an overview of the numerical algorithm used in the present thesis to simulate mixing in curved pipes. I will start by describing the main algorithm of the program and then discuss the details of the implementation.

4.1 Basic description of the algorithm

In this work we use a particle method first developed by Lingevitch and Bernoff in 1994, see [11]. The method is called split-step Monte-Carlo method and is particularly robust in the limit of a small diffusion constant. Thus it is very appropriate for the problems that we are considering.

As we mentioned earlier, the mixing process can be characterized as the simultaneous action on the tracer of advection by the flow and molecular diffusion. In the numerical simulation the tracer is modeled as a collection of massless particles. The particles are released at one location in the curved pipe according to a specified initial condition and their spread and position provide information on the spread and position of the tracer. For instance the average position of all the particles gives information on the position of the center of mass for the tracer. Furthermore, if we distribute the particles in bins, we obtain information on the concentration profile of the tracer. Note that in order for the particles to carry significant information about the tracer we require a relatively high number of particles. This class of methods that models diffusion as a random walk and averages a very large number

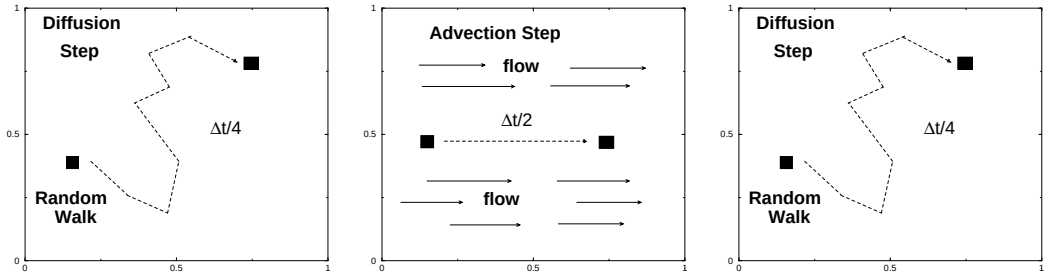

Figure 4.1: This figure illustrate the steps involved in the numerical algorithm used to simulate mixing. Each particle is "mixed" in the following way: the particle takes a random walk for time $t = \Delta t/4$ and this constitute the diffusion step. The particle then follows the flow at that location for time $t = \Delta/2$ and this constitutes the advection step. Finally the particle is diffused for $t = \Delta/4$.

of individual runs to determine the solution goes under the name of Monte-Carlo methods.

The two actions that constitute the mixing process are now characterized in the numerics as an advection step and as a diffusion step. The two actions are performed on a single particle separately according to a specified time step. So if we consider a time step as a unit, we apply diffusion for a quarter of a unit, then apply advection by the flow for half a unit and finally apply diffusion for another quarter of a unit. In the advection step the particle follows the flow at that location. During the diffusion step, the particle reaches a new location with a random walk. This division of steps justifies the "split-step" attribute in the name of the scheme. The two separate steps constitute an accurate representation of the mixing process as they amount to advection for about half of the time and diffusion for another half. Figure 4.1 illustrates the numerical method applied to a single particle. In the following sections we will further analyze the advection and diffusion step.

4.2 Advection step

During the advection step the particles follow the flow at that point for time $\Delta t/2$, where Δt is the length of the time step. In our model of a toroidal pipe the flow is given by a system of first-order differential equations that specify the velocity of the particle, see equations 3.10. In particular the differential equations prescribe the x, y and s components of the velocity. Thus given the initial position p_0 of the particle and the velocities in the various directions, the final position p_1 is obtained by solving an initial value problem. Unfortunately the system of differential equations cannot be solved analytically and we thus need to solve it numerically.

A very naive approach would determine the final position using the so-called Euler's method. This method determines the new position is determined by multiplying the velocity v with the time step Δt to give the total displacement $v\,\Delta t$. We would then add the displacement to the initial position p_0 to give the final position $p_1 = p_0 + v\,\Delta t$. This method seems very promising because the time step in the problem is very small, in the order of $\Delta t = 0.005$. However, this approach is not very robust and leads to significant errors in the order of $(\Delta t)^2 \approx 10^{-6}$. This may seem like a small error but as more time steps are taken the error grows and is expected to grow no worse than linearly with time. Please see [3] p. 262 for a more detailed discussion of the error involved in this method.

A more sophisticated approach determines the final position using the so-called Runge-Kutta method. Here in this thesis we make use of this powerful scheme. This method is more reliable as now the error is of order four. Moreover, to obtain an even better resolution we further divide the interval Δt into 10 smaller steps $\Delta_1 t = \Delta t/10 = 5 \times 10^{-4}$. Thus the total error for every time step in the routine is of the order $(\Delta_1 t)^4 \approx 10^{-16}$. This is a significant improvement on Euler's Method. One may argue that Euler's method could yield a similar accuracy if we choose a small enough time step. However, to obtain the same accuracy we would have

to divide the time step Δt in 10^{10} steps! Thus solving for so many steps would require 10^{10} operations just for one unit of time... The superiority of the Runge-Kutta method is now evident. For more information on the Runge-Kutta method please see [3]. Our implementation follows precisely the implementation for initial value problems discussed in the reference above.

4.3 Diffusion step

During the diffusion step the particles are subject to random walks for a time equivalent to $\Delta t/4$ twice. To explain the action of a random walk, consider a particle at position p_0 at a certain instant in time and after a time $\Delta t/4$, as a result of the random walk, the particle has traveled to a new location p_1. This new position p_1 is related to the initial position p_0 but it is not directly determined by it. Or to better explain we cannot compute directly the new position p_1 from p_0, rather we can only probabilistically predict the new position. This is where the randomness of the process is involved. In fact the new position of the particle is related to the original position through an underlying probability density function (pdf). The pdf specifies how likely it is that a particle will emerge at a given distance from the original location. For random walks in diffusion problems the underlying pdf is always an axisymmetric Gaussian. Technically this condition is referred to as having a Gaussian kernel.

4.3.1 Diffusion in a sheet of water

Before we discuss the details of diffusion in curved pipes, we wish to present an example of this procedure for a set of particles diffusing in an infinite sheet of water. So let $p_0 = (x_0, y_0)$ indicate the initial position of the particle. Our goal is to use the Gaussian kernel to obtain a new position $p_1 = (x_1, y_1)$. Through a random number generator we obtain two random numbers, (r_1, r_2), satisfying the

condition that $0 \leq r_1 \leq 1$ and $0 \leq r_2 \leq 1$. One random number is used to generate the radial displacement of the particle and the second random number to generate the angular displacement. We obtain the radial and angular displacements with the following formulae:

$$R = \sqrt{-4\,D\,\Delta t\,\log(r_1)}$$
$$\theta = 2\,\pi\,r_1.$$

Thus the new positions are:

$$x_1 = R\cos(\theta) + x_0$$
$$y_1 = R\sin(\theta) + y_0.$$

This numerical scheme can model the spreading of particles observed in diffusive processes. Thus if we released $5,000$ particles at the origin of the system, this would correspond to a point like initial condition for the tracer in the sheet of water. The analytical solution for the tracer predicts an axisymmetric Gaussian centered at the origin, spreading across the sheet. Moreover, as time passes the Gaussian becomes wider and wider according to $\sigma = \sqrt{2Dt}$ and shorter and shorter. Under appropriate rescaling, the numerical process yields this result. In fact the particles form a Gaussian distribution and the observed growth-rate σ for the width of the Gaussian is exactly the same as predicted analytically, namely $\sigma = \sqrt{2Dt}$, where D is the diffusion constant.

4.3.2 Diffusion in curved pipes

The numerical scheme implemented to simulate diffusion in a curved pipe uses a similar principle. In our problem diffusion takes place inside a curved pipe. Thus, following the diffusion of a single particle p, we have that after a time Δt, the location of the particle changes from $p_0 = (x_0, y_0, s_0)$ to $p_1 = (x_1, y_1, s_1)$. We cannot determine the displacement directly as was done for diffusion in an infinite sheet.

In fact the coordinate system we use is a cylindrical coordinate system (x, y, s). Thus how can we make the particles "aware" of the curvature of the pipe? A first insight into this problem comes when we notice that the action of a random walk actually ignores the details of the geometry where the particle lives. Effectively diffusion acts in the same way whether the particle is in a cylindrical or curved pipe. Thus we can think of the particle's original location p_0 in the curved pipe. When we apply the random walk, the particle relocates to a new position $p_1' = (x_1', y_1', s_1')$, within the curved pipe. Thus we need to move the particles to the corresponding position p_1 in our representation of the curved pipe. In fact we need to determine the position of the particle in the particular cross-section that goes through p_1'. This is obtained through the following transformation:

$$\begin{aligned} x_1 &= \sqrt{(R + x_1')^2 + (s_1')^2} \; - R + x_0 \\ y_1 &= y_0 + y_1' \\ s_1 &= R \, \mathrm{atan}\left(\frac{s_1'}{R + x_1'}\right) + s_0. \end{aligned} \tag{4.1}$$

The above transformation can be easily derived if we consider the geometry of the problem as illustrated in figure 4.3.2. The figure represents an aerial view of the toroidal pipe with particle taking a random walk from p_0 to p_1. These equations thus permit us to simulate diffusion in a toroidal pipe.

At this point we need to address what would happen if the particle, as a result of a random walk, ends outside the boundaries of the pipe. This is possible since we do not pose any limitation on the distance particles can travel. However, if our model wishes to be an accurate rendition of flows in curved pipes, this is not physically possible because of the solid boundaries. Moreover, as the particles become closer and closer to the boundary it is is very likely that they might diffuse across the boundaries of the pipe. To solve this problem, in our numerical scheme we assume that when a particle hits the wall, it bounces right back without losing any velocity. Numerically we account for this by checking, after the diffusion step, if

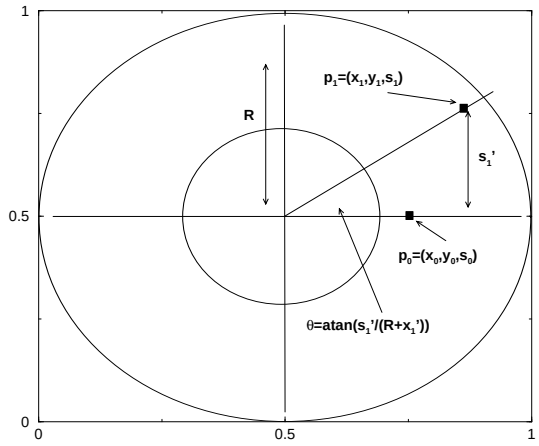

Figure 4.2: This figure represents a particle taking a random walk from the point p_0 to the point p_1. Note that we are taking a view of the toroidal pipe from above. The numerical code assigns new coordinates (x_1', y_1', s_1') as if the particle were in a cylindrical pipe. We then need to express the coordinates in terms of the toroidal pipe's coordinate system. In a toroidal pipe the positions are expressed in terms of the cross-section that passes through the particle p_1' with (x_1, y_1, s_1).

the particle is still inside the cross-section. If it is determined that the particle is outside of the pipe along a cross-section, we reflect the particle across the boundaries of the pipe along that specific cross-section until the particle is back inside.

Chapter 5

Mixing in the toroidal pipe

We are now ready to illustrate in this chapter the main results of this thesis. We begin with a description of the initial condition, the point discharge release at the center of the lobes. We then analyze the growth rate of the cloud of tracer and note that for curved pipes the mixing process displays two anomalous regimes. We then show how the two regimes are consistent with our knowledge for mixing in straight pipes. Finally we end the chapter displaying the longitudinal distribution. These results are consistent with what observed for curved pipe and constitute further evidence for the validity of our analysis.

5.1 Initial conditions: point release at the center of the lobes

For the initial conditions we choose a point release discharge at the center of the lobes. This is the most interesting point release initial condition as a release at the center of the pipe as we saw in figures 3.4 and 3.5 would cause the tracer immediately to accumulate along the boundaries of the pipe. Moreover, this initial condition is the analogous for curved pipes to the centerline release for straight pipes. In Latini and Bernoff, see [9], this yielded the most interesting results and we hope that for curved pipes as well we would observe interesting results. Our objective in fact is to establish an understanding of mixing in terms of different scaling laws for the the spreading of the cloud of tracer as measured by the standard deviation σ. We again wish to construct log-log plots for σ as a function of time. A final consideration that motivates this particular initial condition is the desire to observe a

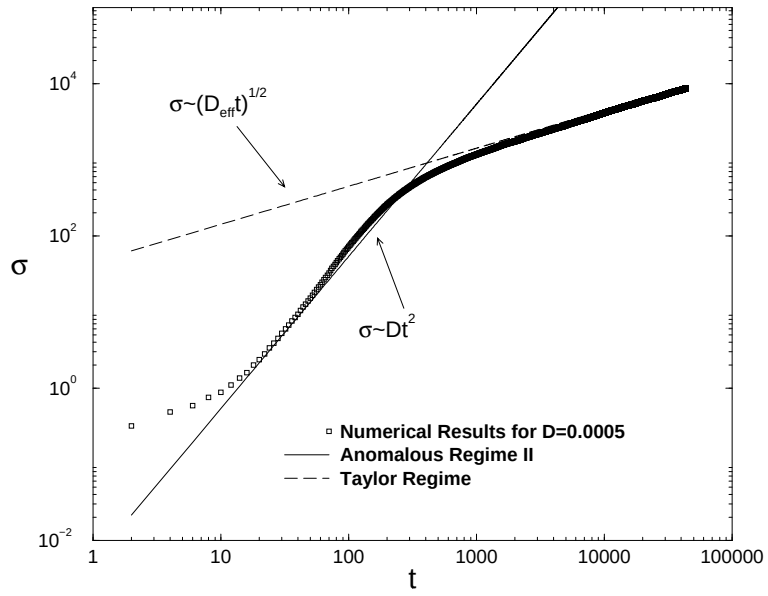

Figure 5.1: In this figure the standard deviation σ is plotted in a log-log scale as a function of time t for a point discharge of tracer at the center of the rotating transversal lobes. The plot clearly indicates two different scaling regimes for σ, the Taylor regime and the anomalous regime. The numerical results are obtained for a value of the diffusivity constant $\mathcal{D} = 0.0005$.

diffusive regime. Thus we consider an initial condition similar to the one that for straight pipes yielded the most visible diffusive regime.

5.2 Anomalous diffusion in curved pipes

Figure 5.1 displays in a log-log plot the width of the cloud of tracer as a function of time for a release at the center of the lobes. The figure displays the width for large times and the two different regimes displayed are the Taylor and the anomalous regime. Thus we have determined the existence of anomalous diffusion in curved pipes.

Now if we consider the scaling laws, we observe something quite peculiar. For large times $\sigma \sim \sqrt{D_{eff} t}$ and this is consistent with Taylor's analysis applied to toroidal pipes. Thus for large times, after the tracer has completely mixed across

the entire cross-section of the pipe, we observe a diffusive growth as a result of the averaging effect. However, for intermediate times we observe a $\sigma \sim Dt^2$ growth. This is a very peculiar result since we would expect a $\sigma \sim D^{1/2}t^{3/2}$ as observed for an off-center release, see figure 2.4. Instead we observe a quadratic growth similar to a centerline release for a straight pipe, see figure 2.2.

This apparent discrepancy can be reconciled with our knowledge of the mixing process. In fact the transverse recirculation generates an effective longitudinal velocity with a quadratic profile centered at the fixed point of the lobes. The particles are spinning around the closed streamlines that constitute the transverse recirculation very rapidly, in time $t_r \approx 3$ as can be seen by the transverse mixing profiles for a uniform strip release on the y-axis, see figures 3.6 and 3.7. Also recall that, because of the parabolic longitudinal velocity profile in curved pipes, particles closer to the center are moving faster longitudinally than particles farther away from the center. Thus for a closed streamline this averages to a net longitudinal velocity along the closed streamline that is less than the longitudinal velocity at the center of the lobes. Thus the effect of the recirculation is to create an effective longitudinal velocity that has two parabolic profiles, one for the upper half of the torus and one for the lower half of the torus. This explains why we observe a t^2 growth in the width of the cloud σ. In this thesis we can only provide a qualitative understanding of these processes. The calculations still need to be explored in full details.

However, we still need to verify the existence of a diffusive regime. Thus we need to concentrate our attention on the growth rate $\sigma(t)$ for small times. The numerical scheme applied to small times generates the profile shown in figure 5.2. This is a most peculiar profile. We clearly see the diffusive regime but we also see a strange "kink" in the growth rate. Before discussing the kink, we acknowledge the diffusive regime. The diffusive regime is consistent with our knowledge of mixing as for very small times the evolution of the dot of tracer can be described

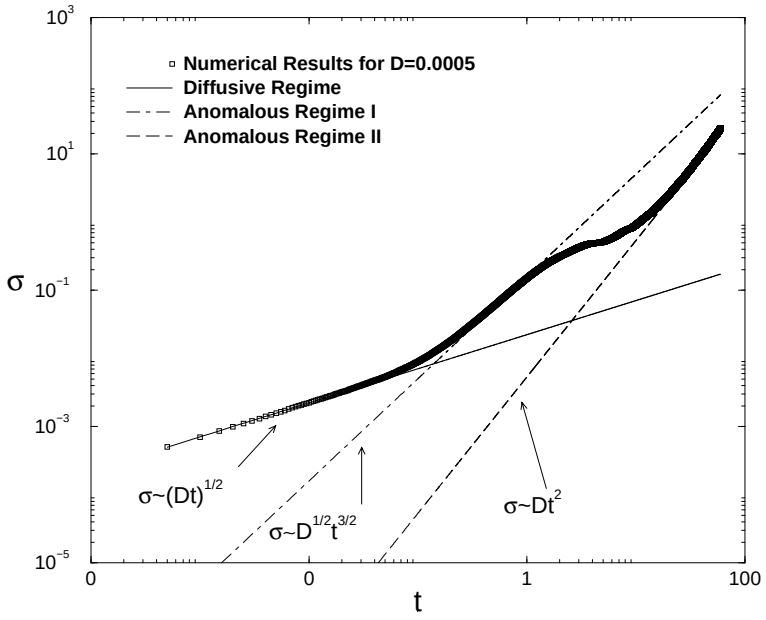

Figure 5.2: In this figure the standard deviation σ is plotted in a log-log scale as a function of time t for a point discharge of tracer at the center of the rotating transversal lobes. The plot clearly indicates three different scaling regimes for σ, the initial diffusive regime and two anomalous regimes. The numerical results are obtained for a value of the diffusivity constant $\mathcal{D} = 0.0005$.

in terms of a diffusion equation translating with the speed of the dot. Now back to the "kink"; is it a physical effect or is it a numerical error? No matter how much the author tried to correct and improve the numerical code to include more particles, or smaller time steps, the kink would not disappear. Thus it could not be a numerical error, but it was perhaps a hallmark of some physical effect. Finally we were able to reconcile the observed phenomenon with our knowledge of mixing.

The kink represents two different anomalous regimes. The first regime, which we call "anomalous I" has scaling law $\sigma \sim D^{1/2}t^{3/2}$ and the second regime, which we call "anomalous II" has scaling law $\sigma \sim Dt^2$. We also note that anomalous I occurs for time less than unity. This provides some insight on the physical processes observed. For very small times the averaging effect is not felt thus the particles "ignore" that they are in a curved pipes and thus they feel the off-center release for

a parabolic velocity profile. Hence anomalous I represents the growth rate as seen in an off-center release for a straight pipe, see figure 2.4. However, as soon as the averaging effect caused by the recirculation is felt, then the particles realize that they are in a curved pipe and that the effective velocity profile is parabolic. This explains the $\sigma \sim t^2$ growth rate in this regime. We were thus able to reconcile our observations with our knowledge of mixing in straight pipes.

There is still one question surrounding the transition between anomalous I and anomalous II. The transition has some bumps. Again these bumps are not caused by numerical error but probably represent some interesting physical effect. We were not able to fully explain this regime and this is one of the open questions of the present work. Another possibility is that the observed regime is just a transition region. In fact notice that, compared to fig. 2.2, the transitions between regimes are here less sharp in curved pipes compared to straight pipes. The transitions seem to occur at a slower rate. This might be connected to the slower cross-mixing compared to the time that it takes for the tracer to complete an entire revolution around the closed streamlines.

5.3 Longitudinal Profiles

We wish to end our analysis with a plot of the longitudinal profiles of the tracer in the various regimes. The figures in 5.3 display the mixing in the cross-section and the longitudinal profiles for the various regimes observed for release at the center of the lobes. In particular the three regimes displayed are the diffusive, anomalous I and anomalous II regimes.

Note that the observed distributions are consistent with what we observe in straight pipes, see fig. 2.3. Thus for both the diffusive and the anomalous I regime, the distribution is Gaussian. In fact anomalous I is equivalent to an off-center release for a straight pipe. Recall that for an off-center release in a straight pipe we

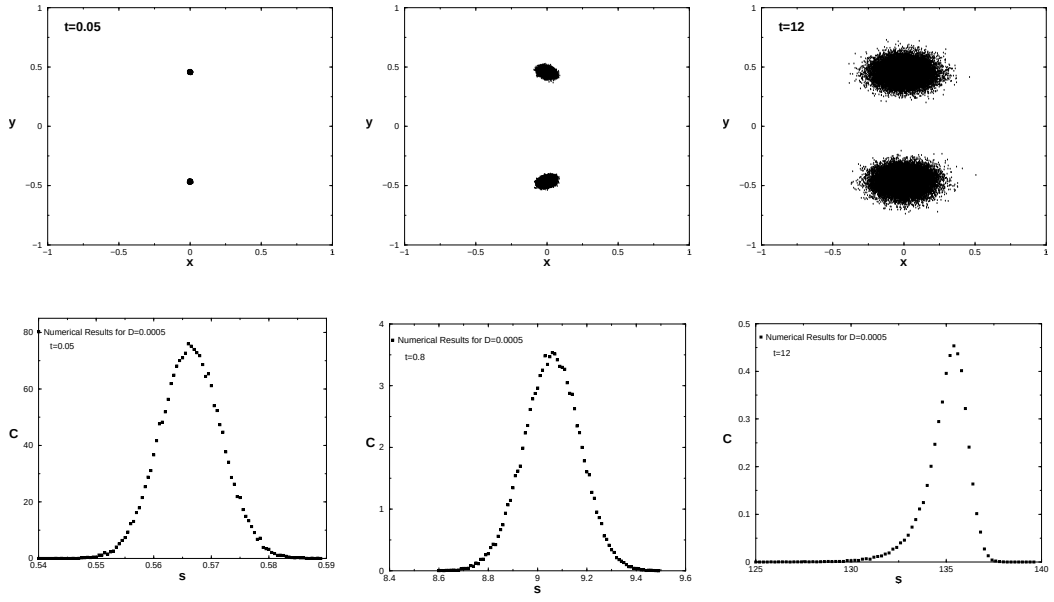

Figure 5.3: The above figures represent the mixing in the cross-section and the longitudinal profiles during the various regimes observed for release of tracer at the center of the lobes. The figure on the left displays the diffusive regime, the central figure displays the anomalous I regime and the figure on the right represents the anomalous II regime.

observe a Gaussian distribution in all three regimes. Also note that for the anomalous II regime we observed an asymmetric profile. This is consistent with what we observe for a center-line release in straight pipes. In fact compare this profile to the profile observed in the anomalous regime for a center-line release in a straight pipe, see fig. 2.4. The two figures are exactly equivalent and this constitutes further confirmation to our analysis. This is one of the most promising result of this thesis. In fact we can now easily describe the longitudinal profiles observed for mixing in curved pipes in terms of the profiles observed for mixing in straight pipes.

Chapter 6

Conclusions & Future Work

I wish to summarize in this chapter our major findings in this thesis. I also wish to outline some future work that I wish to pursue on this problem and pose some questions that still need to be answered.

6.1 Results

In this thesis we analyzed mixing in curved pipes. In a toroidal pipe, the curvature induces in the flow a transverse recirculation in the form of outward spinning vortices first predicted by Dean in 1928, see [5]. We released tracer at the center of the rotating lobes and plotted the longitudinal growth rate σ of the cloud of tracer as a function of time. We were able to identify four regimes that characterize the mixing process. For very small times we observed a diffusive regime with $\sigma \sim \sqrt{Dt}$ since the evolution of the cloud of tracer can be described by a diffusion equation translating with the velocity of the dot of tracer. For intermediate times we observed two anomalous regimes. The first anomalous regime, which we called anomalous I, displayed a growth rate $\sigma \sim D^{1/2}t^{3/2}$. This finding is consistent with our results for an off-center release in straight pipes, see [9]. In fact for small times the particles do not know that they are in a curved pipe. This regime is immediately followed by a second anomalous regime, which we called anomalous II, with $\sigma \sim Dt^2$. This regime thus displays the characteristics of a centerline release for a straight pipe. This is consistent with our theory because the recirculation averages the longitudinal velocities around the closed streamlines causing an effective parabolic velocity

profile. Finally, for large times, we observed the Taylor regime with $\sigma \sim \sqrt{D_{eff}t}$. This regime is consistent with our theory and is achieved after the particles have completely mixed across the entire cross-section of the pipe.

We also plotted the longitudinal concentration profiles and our findings are consistent with what observed for straight pipes. Thus we observed a Gaussian longitudinal distribution for the diffusive, anomalous I, and Taylor regime. For the anomalous II regime we observed an asymmetric distribution which is similar to what observed for curved pipes.

This summarizes the major findings for this thesis. We were able in the present work to extend our results for straight pipes to include the toroidal pipe. Moreover, we elucidated some of the basic processes involved in mixing for curved pipes drawing on familiar results for straight pipes.

6.2 Future work

I wish to briefly discuss in this section some of the work I would like to pursue to further elucidate processes described in this thesis.

First of all I would like to find a further foundation to the claims that we have made in this thesis. Thus derive analytically the constants that govern the various regimes. In fact we found the correct scaling but we need to understand the dependence of such scaling on the various parameters. This result would then immediately enable to find the equations for the various profiles.

The dependence on the constants further suggest another problem that needs to be solved and this is the number of parameters in the problem. Right now the problem has three parameters: D, the diffusion constant, α and β used in equations 3.10 for the velocities in the cross-section. However, we suspect that the problem may depend only on two parameters, D and some combination of α and β. Thus one may try to determine if the problem can be further simplified to two parame-

ters.

Another interesting question is trying to determine if the strange wiggles observed in fig. 5.2 during the transition from anomalous I to anomalous II are the hallmark of some physical process that needs to be elucidated or instead represent just some interesting transition pattern from the various regimes.

Finally an interesting generalization of this problem, would be to extend this theory to understand mixing in helical pipes and more generally to other more complex geometries.

Bibliography

[1] R. Aris. On the dispersion of a solute in a fluid flowing through a tube. *Proc. Roy. Soc. London Ser. A*, 235:67–77, 1956.

[2] S. A. Berger, L. Talbot, and L. S. Yao. Flow in curved pipes. *Ann. Rev. Fluid Mech.*, 15:461–512, 1983.

[3] Richard L. Burden and J. Douglas Faires. *Numerical Analysis*. Brooks/Cole Publishing Company, Pacific Grove, California, 1997.

[4] W. R. Dean. Note on the motion of fluid in a curved pipe. *Phil. Mag.*, 4(20):208–223, 1927.

[5] W. R. Dean. The steam-line motion of fluid in a curved pipe. *Phil. Mag.*, 5(30):673–693, 1928.

[6] M. Germano. On the effect of torsion on a helical pipe flow. *J. Fluid Mech.*, 125:1–8, 1982.

[7] M. Germano. The dean equations extended to a helical pipe flow. *J. Fluid Mech.*, 203:289–305, 1989.

[8] Scott W. Jones, Oran M. Thomas, and Hassan Aref. Chaotic advection by laminar flow in a twisted pipe. *J. Fluid Mech.*, 209:335–357, 1989.

[9] Marco Latini and Andrew J. Bernoff. Transient anomalous diffusion is poiseuille flow. *preprint*.

[10] M. J. Lighthill. Initial development of diffusion in poiseuille flow. *J. Inst. Math. Appl.*, 2:97–108, 1966.

[11] Joseph F. Lingevitch and Andrew J. Bernoff. Advection of a passive scalar by a vortex couple in the small-diffusion limit. *J. Fluid Mech.*, 270:219–249, 1994.

[12] T. J. Pedley. *The fluid mechanics of large blood vessels*. Cambridge University Press, New York, 1980.

[13] P. B. Rhines and W. R. Young. How rapidly is a passive scalar mixed within closed streamlines? *J. Fluid Mech.*, 133:133–145, 1983.

[14] G. I. Taylor. Dispersion of a soluble matter in solvent flowing slowly through a tube. *Proc. Roy. Soc. London Ser. A*, 219:186–203, 1953.

[15] Eric R. Weeks, J. S. Urbach, and Harry L. Swinney. Anomalous diffusion in asymmetric random walks with a quasi-geostrophic flow example. *Phys. D*, 97:291–310, 1996.